Fractal Growth Phenomena

Tamás Vicsek

Institute for Technical Physics
Budapest, Hungary

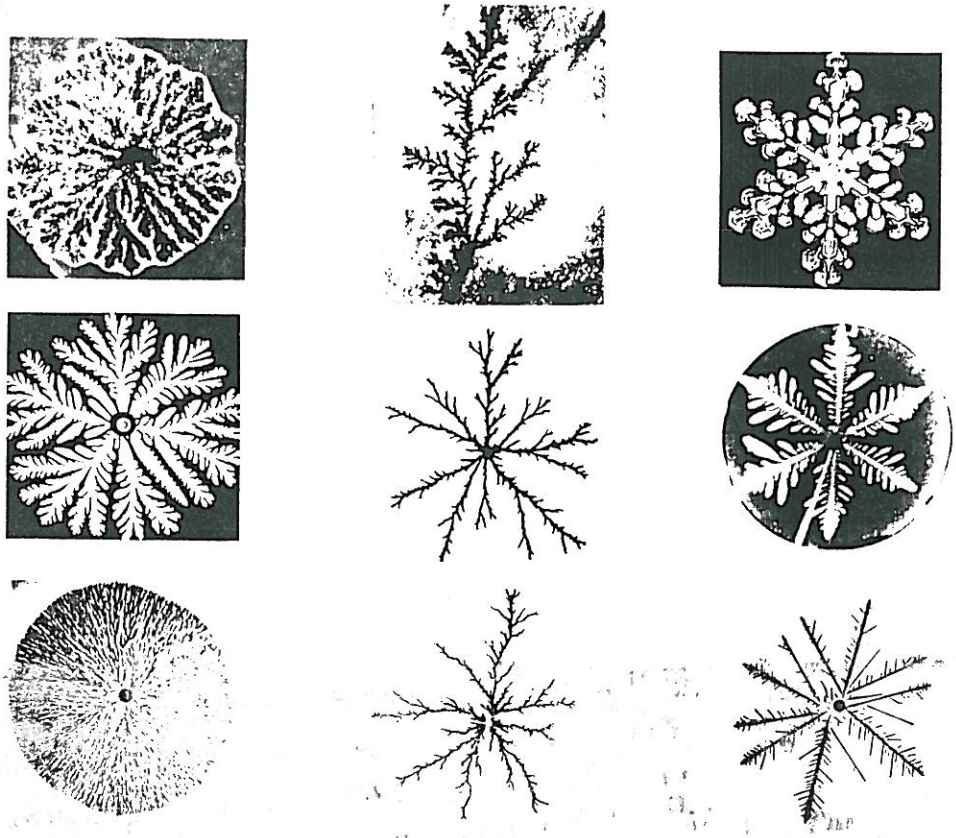

WORLD SCIENTIFIC
Singapore

$D = A \cdot b^{\alpha}$

$C(r) \sim A r^{\alpha} \quad r \to br \quad C(br) \sim D r^{\alpha}$

Scaling, new-analitikus, kritikus viselkedés, kritikus pont univerzális kritikus exponensek

PART I.

FRACTALS

Chapter 2.

FRACTAL GEOMETRY

Our present knowledge of fractals is a result of an increasing interest in their behaviour. Some of the basic properties of objects with anomalous dimension were noticed and investigated at the beginning of this century mainly by Hausdorff (1919) and Besicovich (1935). The relevance of fractals to physics and many other fields was pointed out by Mandelbrot, who demonstrated the richness of fractal geometry and presented further important results in his recent books on the subject (Mandelbrot 1975, 1977 and 1982). The purpose of this chapter is to give an introduction to the basic concepts, properties and types of fractals.

2.1. FRACTALS AS MATHEMATICAL AND PHYSICAL OBJECTS

One of the common features of fractal objects is that they are *self-similar* (scale invariant). This means that if we first cut out a part of them, and then we blow this piece up, the resulting object (in a statistical sense) will look the same as the original one. For example, if we took a picture of the shore of England from an airplane we would get a curve with an overall appearance rather similar to another picture which we would see when standing on the ground and looking at a rocky part of the shore. Analogously, a bough with lateral branches looks like the whole tree when looked at from a larger

distance. For simpler shapes, self-similarity is not fulfilled or it is satisfied in a trivial way. A circle and its parts (the arcs) do not look the same, but naturally, a filled circle (a disc) and any smaller disc cut out of it are trivially similar (can be obtained from each other by reduction or extension).

Another typical property of fractals is related to their volume with respect to their linear size. To demonstrate this we first need to introduce a few notions. We call *embedding dimension* the Eucledian dimension d of the space the fractal can be embedded in. In addition, d has to be the smallest such dimension. Obviously, the volume of a fractal (or any object), $V(l)$, can be measured by covering it with d dimensional balls of radius l. Then the expression

$$V(l) = N(l)l^d \tag{2.1}$$

gives an estimate of the volume, where $N(l)$ is the *number of balls needed to cover the object completely* and l is much smaller than the linear size L of the whole structure. The structure is regarded to be covered if the region occupied by the balls includes it entirely. The phrase "number of balls needed to cover" corresponds to the requirement that $N(l)$ should be the smallest number of balls with which the covering can be achieved. For ordinary objects $V(l)$ quickly attains a constant value, while for fractals typically $V(l) \to 0$ as $l \to 0$. On the other hand, the surface of fractals may be anomalously large with respect to L.

There is an alternative way to determine $N(l)$ which is equivalent to the definition given above. Consider a d-dimensional hypercubic lattice of lattice spacing l which occupies the same region of space where the object is located. Then the number of boxes (mesh units) of volume l^d which overlap with the structure can be used as a definition for $N(l)$ as well. This approach is called *box counting*.

Returning to the example of the shore of England we can say that it can be approximately embedded into a plane ($d = 2$). Measuring its total length (corresponding to the surface in a two-dimensional space) we would find that it tends to grow almost indefinitely with the decreasing length l of

the measuring sticks. At the same time, the measured "area" of the shore (volume in $d = 2$) goes to zero if we determine it by using discs of decreasing radius. The reason for this is rooted in the extremely complicated, self-similar character of the shore. Therefore, such a curve seems to be definitely much "longer" than a line but having infinitely small area: it is neither a one- nor a two dimensional object.

We have seen on the example of the shore that the volume of a finite geometrical structure measured according to eq. (1) may go to zero with the decreasing size of the covering balls while, simultaneously, its measured surface diverges. In general, we *call a physical object fractal, if measuring its volume, surface or length with* d, $d-1$ *etc. dimensional hyperballs it is not possible to obtain a well converging finite measure for these quantities when changing* l *over several orders of magnitude.*

It is possible to construct mathematical objects which satisfy the criterion of self-similarity exactly, and their measured volume depends on l even if l or (l/L) becomes smaller than any finite value. Fig. 2.1 gives examples how one can construct such fractals using an iteration procedure. Usually one starts with a simple initial configuration of units (Fig. 2.1a) or with a geometrical object (Fig. 2.1b). Then, in the growing case this simple seed configuration (Fig. 2.1a, $k = 2$) is repeatedly added to itself in such a way that the seed configuration is regarded as a unit and in the new structure these units are arranged with respect to each other according to the same symmetry as the original units in the seed configuration. In the next stage the previous configuration is always looked at as the seed. The construction of Fig. 2.1b is based on division of the original object and it can be well followed how the subsequent replacement of the squares with five smaller squares leads to a self-similar, scale invariant structure.

One can generate many possible patterns by this technique; the fractal shown in Fig. 2.1 was chosen just because it has an open branching structure analogous to many observed growing fractals (Vicsek 1983). Only the first couple of steps (up to $k = 3$) of the construction are shown. *Mathematical fractals* are produced after *infinite number of such iterations.* In this $k \to \infty$ limit the fractal displayed in Fig. 2.1a becomes infinitely large, while the

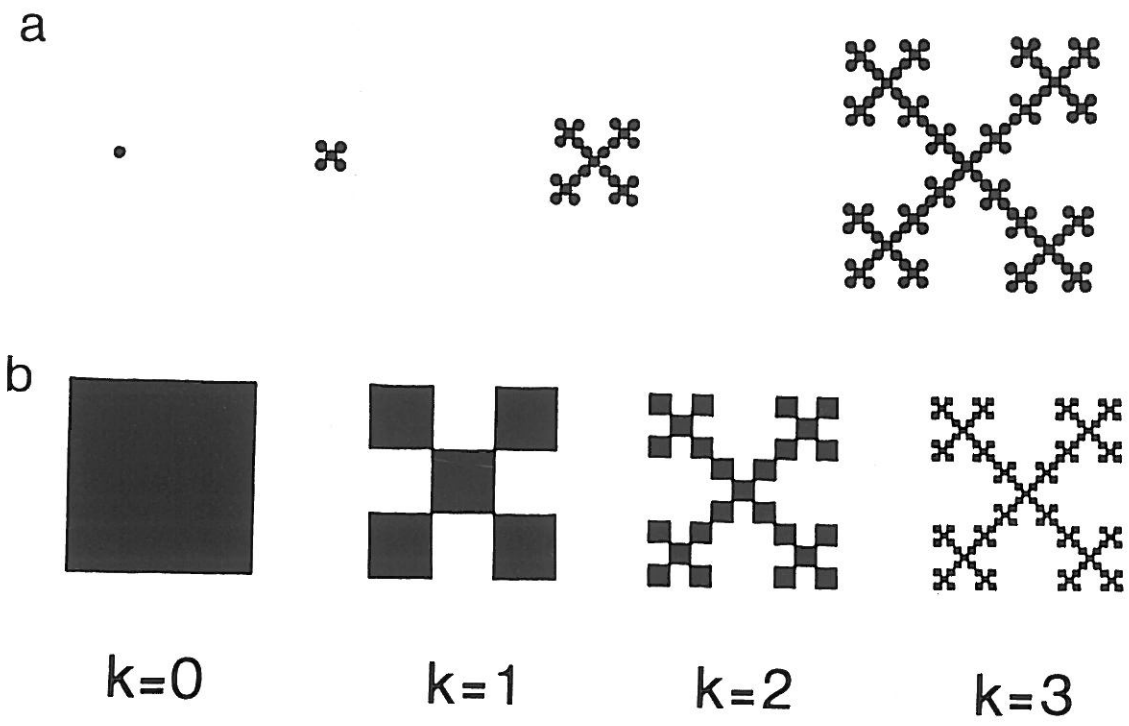

Figure 2.1. Example for the construction of a deterministic fractal embedded into two dimensions. Fig. 2.1a demonstrates how one can generate a growing fractal using an iteration procedure. In Fig. 2.1b an analogous structure is constructed by subsequent divisions of the original square. Both procedures lead to fractals for $k \to \infty$ with the same dimension $D \simeq 1.465$.

details of Fig. 2.1b become so fine that the picture seems to "evaporate" and can not be seen any more. For every finite k the structures in Fig. 2.1a can be scaled into each other, but this can not be done exactly in the $k \to \infty$ limit. Our example shows a connected construction, but disconnected objects distributed in a nontrivial way in space can also form a fractal.

There are a few important things to be pointed out in connection with Fig.2.1. and fractal growth phenomena. Obviously, it is Fig. 2.1a which better approximates a real growth process. In a physical system there is always a lower cutoff of the length scale; in our case this is represented by the size of the particles. On the other hand a real object has a finite linear size which inevitably introduces an upper cutoff of the scale on which fractal scaling can be observed. This leads us to the conclusion that, in contrast

to the mathematical fractals, for fractals observed *in physical phenomena the anomalous scaling of the volume can be observed only between two well defined length scales.* For growing fractals the volume is usually measured as a function of increasing linear size of structure.

There is a widely studied phenomenon in which the second type of fractals (Fig. 2.1b) play an essential role. It can be shown that in chaotic dissipative systems the trajectories in the phase space approach a fractal called strange attractor. In this case the fractal object is both finite and mathematical; it has infinitely fine details. It is a general belief that chaos and fractal growth are closely related, but the two fields have not been included into a unified picture yet.

2.2. DEFINITIONS

Since measuring the volume of fractals embedded into a d dimensional Eucledian space leads to the conclusion that they are objects having no integer dimension, we assume that the dimensionality of fractals is usually given by a noninteger number D that will be called fractal dimension. Because of the two main types of fractals demonstrated in Fig. 2.1, to define and determine D one typically uses two related approaches.

In the case of growing fractals, where there exists a smallest typical size a, one cuts out d-dimensional regions of linear size L from the object and the volume, $V(L)$, of the fractal within these regions is considered as a function of the linear size L of the object. When determining $V(L)$, the structure is covered by balls or boxes of unit volume ($l = a = 1$ is usually assumed), therefore $V(L) = N(L)$, where $N(L)$ is the number of such balls. In some cases this definition has to be modified to obtain consistent results (Tél and Vicsek 1987). According to the modification one requires that the size of the covering balls has to diverge as well, i.e., $a/l \to 0$ and $l/L \to 0$ should be satisfied when $L \to \infty$ (see Section 3.4.)

For fractals having fixed L and details on very small length scale D is defined through the scaling of $N(l)$ as a function of decreasing l, where

$N(l)$ is the number of d dimensional balls of diameter l needed to cover the structure. The fact that an object is a mathematical fractal then means that $N(l)$ diverges as $L \to \infty$ and $l \to 0$, respectively, according to a non-integer exponent. Correspondingly,

$$N(L) \sim L^D \tag{2.2}$$

and

$$D = \lim_{L \to \infty} \frac{\ln N(L)}{\ln(L)} \tag{2.3}$$

for the *growing case*, where $l = 1$. Here, as well as in the following expressions the symbol $\sim$ means that the proportionality factor, not written out in (2.2), is independent of ϵ. For fractals having a finite size and infinitely small ramifications we have

$$N(l) \sim l^{-D} \tag{2.4}$$

with

$$D = \lim_{l \to 0} \frac{\ln N(l)}{\ln(1/l)}. \tag{2.5}$$

Obviously, the above definitions for non-fractal objects give a trivial value for D coinciding with the embedding Eucledian dimension d. For example, the area (corresponding to the volume $V(L)$ in $d = 2$) of a circle grows as its squared radius which according to (2.3) results in $D = 2$. Similarly, the number of circles needed to cover a square diverges as the inverse of the squared radius of these circles leading again to $D = d = 2$ on the basis of (2.5).

Now we are in the position to calculate the dimension of the objects shown in Fig. 2.1. It is evident from the figure that for the growing case

$$N(L) = 5^k \qquad \text{with} \qquad L = 3^k, \tag{2.6}$$

where k is the number of iterations completed. From here using (2.3) we get the value $D = \ln 5/\ln 3 = 1.465...$ which is a number between $d = 1$ and $d = 2$ just as we expected. Analogously, for the fractal shown in Fig. 2.1b $N(l) = 5^k$ with $l = 3^{-k}$, leading to the same D.

Non-trivial self-similarity and the fractal value for the dimensionality of the objects are closely related. This can be seen from the fact that $D < d$ results in a negligible volume in the d dimensional embedding space. For growing fractals $V(L)/L^d \to 0$ as $L \to \infty$ means that the structure must possess large empty regions (holes) with diameters comparable to its actual linear size L. It is the presence of holes on every length scale which is the origin of non-trivial scale invariance.

In the previous paragraph we made use of the fact that the object we considered had a lower (the size of the particles) and an upper cutoff length scale (the size of the whole structure). This is, however, a property we can assume for all objects arising as a result of any physical process. The finite size ($L < \infty$) of physical fractals makes it possible to treat all of the physically relevant cases using a dimensionless quantity

$$\epsilon = \frac{l}{L} \tag{2.7}$$

which is the size of covering balls normalized by the linear size of the structure. In the case of growing fractals when the fractal dimension is investigated l (the size of the particles) is kept constant and L is increasing, while for fractals generated by subsequent divisions L is constant and l is decreasing. Therefore, (2.2) and (2.4) in terms of ϵ are recast into the same form

$$N(\epsilon) \sim \epsilon^{-D}, \tag{2.8}$$

where $\epsilon \ll 1$, $N(\epsilon)$ is the number of d dimensional balls of radius ϵL needed to cover the fractal, and D is the same fractal dimension as in (2.2) and (2.4).

In the following when discussing properties of fractals in general, we shall use (2.8), while in the case of describing various particular growth processes it is more convenient to apply expression (2.2). A definition analogous to (2.8) was first used to determine a non-integer dimension for geometrically very complex objects by Hausdorff (1919) and later put into a more systematic framework by Besicovitch (1935). In fact, the definitions given by them are more general than the above expression and contain (2.8) as a special case. Eq. (2.8) is more directly related to the Kolmogorov capacity (Kolmogorov and Tihomirov 1959).

The original intention of Hausdorff was to define a measure being independent of the resolution of the measurement, ϵ. We have seen that for non-trivially self-similar objects measuring the volume with balls of integer dimension, it goes either to zero or to infinity. This problem was avoided by Hausdorff who suggested that the volume should be measured covering the structure with ordinary balls, but assuming that the volume or measure of a ball is ϵ^D. Then the so called Hausdorff measure is calculated according to

$$F = N(\epsilon)\epsilon^D. \tag{2.9}$$

It can be seen easily from (2.8) that F is independent of ϵ then, and only then if D, the assumed dimension of the balls, coincides with the fractal dimension D of the object studied.

To conclude this section *ordinary fractals are defined as objects for which D determined from (2.8) is smaller than the embedding dimension d.* This definition, however, should be completed by a few remarks. For physical fractals (2.8) holds only within a few magnitudes of changing ϵ. In addition, as we shall see later, there are objects (called fat fractals) for which $D = d$, but share some of the properties of ordinary fractals. Namely, when measuring their finite volume one obtains a correction converging to zero very slowly (according to a power law, just as the total volume of an ordinary fractal).

USEFUL RULES

Before reviewing some of the most typical types of the rich botanic garden of fractals we mention a few rules which can be useful in predicting various properties related to the fractal structure of an object. Of course, because of the great variety of self-similar geometries the number of possible exceptions is not small and the rules listed below should be regarded, at least in part, *as* starting points for more accurate conclusions.

a) Many times it is the *projection* of a fractal which is of interest or can be experimentally studied (e.g., a picture of a fractal embedded into $d = 3$). ln general, projecting a $D < d -$ m dimensional fractal onto a $d -$ m dimensional surface results in a structure with the same fractal dimension $Dp = D$. For D 2: $d -$ m the projection fills the surface, $Dp = d - m$.

b) It follows from a) that for $D < d$ -m the density correlations e(r) (see the next section) within the projected image decay *as* a power law with an exponent $d -$ m $- D$ instead of $d - D$ which is the exponent characterizing the algebraic decay of c(r) in d.

e) Cutting out a d -m dimensional slice (*cross section)* of a D dimensional fractal embedded into a d dimensional space usually leads to a $D -$ m dimensional object. This seems to be true for self-affine fractals *as* well, with D being their local dimension (see Section 2.3.2).

d) Consider two sets A and B having fractal dimensions DA and DB, respectively. *Multiplying* them together results in a fractal with $D = DA + DB$. As a simple example, imagine a fractal which is made of parallel sticks arranged in such a way that its cross section is the fractal shown in Fig. 2.lb. The dimension of this object is $D = 1 + \ln 5 / \ln 3$.

e) The *union* of two fractal sets A and B with $DA > DB$ has the dimen- sion $D = DA$.

f The fractal dimension of the *intersection* of two fractals with DA and DB is given by $DAnB = DA + DB - d$. To see this, consider a box of

linear size L within the overlapping region of two growing stochastic fractals. The density of A and B particles is respectively proportional to L^{D_A}/L^d and L^{D_B}/L^d. The number of overlapping sites $N \sim L^{D_{A\cap B}}$ is proportional to these densities and to the volume of the box which leads to the above given relation. The rule concerning intersections of fractals with smooth hypersurfaces is a special case of the present one.

g) The distribution of empty regions (holes) in a fractal of dimension D scales as a function of their linear size with an exponent $-D-1$. The following heuristic argument supporting the above result is here applied to the one-dimensional case. The statement is essentially the following

$$n(\epsilon, \Delta\epsilon) \sim \epsilon^{-D-1}\Delta\epsilon,$$

where $n(\epsilon, \Delta\epsilon)$ is the number of gaps (empty regions) of length between ϵ and $\epsilon - \Delta\epsilon$. This can be seen by noting that the total length covered with intervals ϵ is

$$L(\epsilon) \sim \epsilon^{-D+1}.$$

The increase of the uncovered part when ϵ is decreased to $\epsilon - \Delta\epsilon$ is

$$\frac{dL(\epsilon)}{d\epsilon}\Delta\epsilon \sim \epsilon^{-D}\Delta\epsilon.$$

This comes from the gaps of length between ϵ and $\epsilon - \Delta\epsilon$, because they will not be covered any more. Thus,

$$\epsilon^{-D}\Delta\epsilon \sim n(\epsilon, \Delta\epsilon)\epsilon\Delta\epsilon$$

which is equivalent to the statement.

2.3. TYPES OF FRACTALS

One of the most fascinating aspects of fractals is the extremely rich variety of possible realizations of such geometrical objects. This fact raises the question of classification, and in the book of Mandelbrot (1982) and in the following publications many kinds of fractal structures have been described. Below we shall discuss a few important classes with some emphasis on their relevance to growth phenomena.

2.3.1. Deterministic and random fractals

Since fluctuations are always present in physical processes, they never lead to structures with perfect symmetry. Instead, physical fractals are more or less random with no high level of symmetry. Yet it is of interest to investigate simple, idealized fractal constructions, because the main features of fractal geometry can be effectively demonstrated using them as examples.

Fig. 2.1a shows a typical fractal generated by a *deterministic rule.* In general when constructing such *growing mathematical fractals* one starts with an object (particle) of linear size a. In the first step ($k = 1$) $n - 1$ copies of this seed object are added to the original one so that the linear size of the resulting configuration become ra, where $r > 1$. Next ($k = 2$) each particle in the first configuration is substituted by the whole $k = 1$ configuration itself. In this way the number of particles and the linear size of the structure becomes n^2 and r^2a, respectively. In the kth step the same rule is applied: each particle is replaced by the $k = 1$ configuration. Similarly, the kth configuration is made of n units being identical to the $k - 1$th cluster. In other words, when making the $k + 1$th step the n subunits of the kth configuration corresponding to the structure obtained in the $k - 1$th step are replaced by the structure generated in the kth stage of this iteration procedure. The $k \to \infty$ limit results in a deterministic mathematical fractal. At the end of this section a few examples are given for the types of fractals described above and in the following.

The fractal dimension for such objects can readily be obtained from

(2.3). Taking into account that for $L = r^k a$ the volume (the number of particles) of the structure is $N(L) = n^k$, we get

$$D = \frac{\ln n}{\ln r} \tag{2.10}$$

which is an exact expression for D.

The construction of deterministic fractals generated by subsequent *divisions* of a starting object proceeds in an analogous manner. In the first step this object having a linear size $L_0 = 1$ is divided into n identical parts each of which is a reduced version of the original structure with the same factor $1/r$. During the next step n copies of the starting object reduced by a factor $(1/r)^2$ are arranged inside a part generated in the previous step. This is done in a way which exactly corresponds to the arrangement of the parts placed in the first step within the object. In this case each of the n^k objects obtained in the kth step is replaced by the $k = 1$ configuration reduced by a factor of $(1/r)^k$. It is obvious that the number of balls of radius $\epsilon = (1/r)^k$ needed to cover the structure grows with k as n^k which on the basis of (2.4) leads to the expression (2.10) for the fractal dimension.

As was mentioned earlier, the two methods of generating deterministic fractals are closely related. For every finite k the linear size of a growing fractal can be rescaled to the same value L_0 and the objects obtained in this way are the same as those generated by subsequent divisions using the appropriate rule. Thus, for the sake of simplicity, in the following we shall mainly use the language corresponding to the method of divisions.

The above described constructions lead to uniform fractals in the sense that we used the same reduction parameter for all of the copies made. An important generalization of these is represented by the case when the reduction factor $(1/r)$ is not identical for all of the n newly created copies within the parts generated in the previous step of the procedure. As before, the fractal is produced by dividing an original object into parts being reduced versions of it, but this time the factors $r_i > 1, (i = 1, 2, ...n)$ can not be all identical. Such non-uniform fractals are obtained in the limit of repeating the iteration procedure infinitely many times (see the examples at the end

of this section).

To determine the fractal dimension of a *non-uniform* mathematical fractal we first note that it can be devided into n parts each being a rescaled version of the complete fractal. Let $N_i(\epsilon)$ denote the number of balls of radius ϵ needed to cover the ith part. The number of balls needed to cover the whole fractal is

$$N(\epsilon) = \sum_{i=1}^{n} N_i(\epsilon). \tag{2.11}$$

Since the fractal is self-similar,

$$N_i(\epsilon/r_i) = N(\epsilon) \tag{2.12}$$

expressing the fact that one needs the same number of balls of reduced radius ϵ/r_i to cover a smaller version of the fractal of size L_0/r_i, than one needs for covering the complete structure with balls of radius ϵ. Then substitution of (2.4) and (2.12) into (2.11) leads to

$$\sum_{i=1}^{n} \left(\frac{1}{r_i}\right)^{D} = 1 \tag{2.13}$$

which is an implicit equation for the fractal dimension of non-uniform fractals. For $r_i = r_1 = r_2 = ... = r_n$, (2.13) is equivalent to (2.10).

Although in the following chapters we shall concentrate on the study of *random fractals* growing in physical processes, here we first show that one can generate simple stochastic fractals in a way analogous to the above described constructions. To take an example let us consider the fractal shown in Fig. 2.1b. It is constructed by dividing the original square into 9 equal parts and deleting 4 of them selected randomly (i.e. keeping 5). In the following steps the same procedure is repeated with the remaining squares. Fig. 2.2 shows the resulting structure after 3 iterations. Comparing the geometrical appearance of Fig. 2.1b and 2.2 we find that they are quite different, however, their fractal dimension is identical $D = \ln 5/\ln 3 = 1.465...$, because one

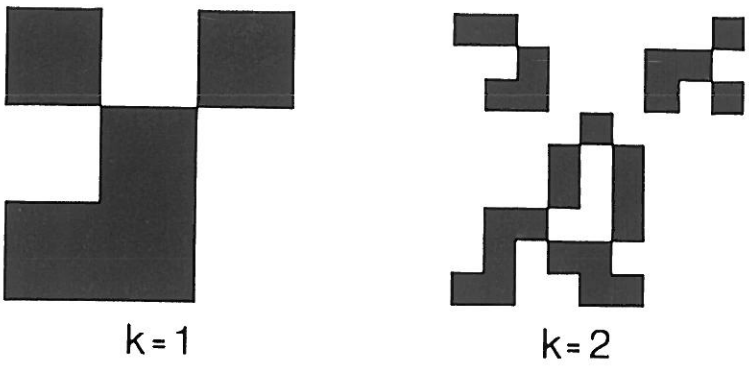

Figure 2.2. Construction of a stochastic fractal. Its fractal dimension is exactly the same as that of the structure shown in Fig. 2.1, despite the fact that they look quite different.

needs the same number of balls to cover them.

Of course, this construction represents only a simple (perhaps the simplest) version of possible random fractals. For example, it is not only the position of the reduced parts which can be varied, but the number of such units and/or the reduction parameter can also fluctuate around their average value. In general, for the fractal dimension of random fractals an explicit expression analogous to (2.10) does not exist and D has to be determined using various theoretical and numerical techniques which will be discussed in Chapter 4.

Self-similarity can be directly checked for a deterministic fractal constructed by iteration, but in the case of random structures one needs other methods to detect the fractal character of a given object. In fact, *random fractals are self-similar only in a statistical sense* (not exactly) and to describe them it is more appropriate to use the term scale invariance than self-similarity. Naturally, for demonstrating the presence of fractal scaling one can use the definition based on covering the given structure with balls of varying radii, however, this would be a rather troublesome procedure. It is more effective to calculate the so called *density-density or pair correlation function*

$$c(\vec{r}) = \frac{1}{V} \sum_{\vec{r}'} \rho(\vec{r} + \vec{r}')\ \rho(\vec{r}') \tag{2.14}$$

which is the expectation value of the event that two points separated by $\vec{r}$ belong to the structure. For growing fractals the volume of the object is $V = N$, where N is the number of particles in the cluster, and (2.14) gives the probability of finding a particle at the position $\vec{r} + \vec{r}'$, if there is one at $\vec{r}'$. In (2.14) ρ is the local density, i.e., $\rho(\vec{r}) = 1$ if the point $\vec{r}$ belongs to the object, otherwise it is equal to zero. Ordinary fractals are typically isotropic (the correlations are not dependent on the direction) which means that the density correlations depend only on the distance r so that $c(\vec{r}) = c(r)$.

Now we can use the pair correlation function introduced above as a criterion for fractal geometry. An object is non-trivially scale-invariant if its correlation function determined according to (2.14) is unchanged up to a constant under rescaling of lengths by an arbitrary factor b:

$$c(br) \sim b^{-\alpha} c(r) \tag{2.15}$$

with α a non-integer number larger than zero and less than d. It can be shown that the only function which satisfies (2.15) is the power law dependence of $c(r)$ on r

$$c(r) \sim r^{-\alpha} \tag{2.16}$$

corresponding to an algebraic decay of the local density within a random fractal, since the pair correlation function is proportional to the density distribution around a given point. This fact can be used for expressing the fractal dimension through the exponent α. To show this for growing fractals, we calculate the number of particles $N(L)$ within a sphere of radius L from their density distribution

$$N(L) \sim \int_0^L c(r) d^d r \sim L^{d-\alpha}, \tag{2.17}$$

where the summation in (2.14) has been replaced by integration. Comparing (2.17) with (2.2) we arrive at the desired relation

$$D = d - \alpha \tag{2.18}$$

which is a result widely used for the determination of D from the density correlations within a random fractal.

EXAMPLES

Next we give a few characteristic examples for the types of fractals mentioned in this section to illustrate the basic ideas discussed above. Because of the great variety of possible constructions the list is far from being complete, and those readers who are interested in more examples are advised to consult the book of Mandelbrot (1982).

Example 2.1. One of the simplest and best known fractals is the so called triadic Cantor set which is a finite size fractal consisting of disconnected parts embedded into one-dimensional space ($d = 1$). Its construction based on the subsequent division of intervals generated on the unit interval $[0, 1]$ is demonstrated in Fig. 2.3. First $[0, 1]$ is replaced by two intervals of length $1/3$. Next this rule is applied to the two newly created intervals, and the procedure is repeated *ad infinitum*. As a result we obtain a deterministic fractal and to calculate its fractal dimension we can use Eq. (2.10). Obviously, for the present example $n = 2$ and the reduction factor is $1/r = 1/3$. Therefore (2.10) gives for the dimension of the triadic Cantor set $D = \ln 2 / \ln 3 = 0.6309...$ which is a rational number less than 1. In general, Cantor sets with various n and r can be constructed. For example, keeping $n = 2$ and changing r between 2 and ∞ any fractal dimension $0 \leq D \leq 1$ can be produced. On the other hand, various Cantor sets with the same fractal dimension can be constructed as well. The two sets $n = 2$, $r = 4$ and $n = 3$, $r = 9$ have the same fractal dimension $D = 1/2$, but different overall appearance.

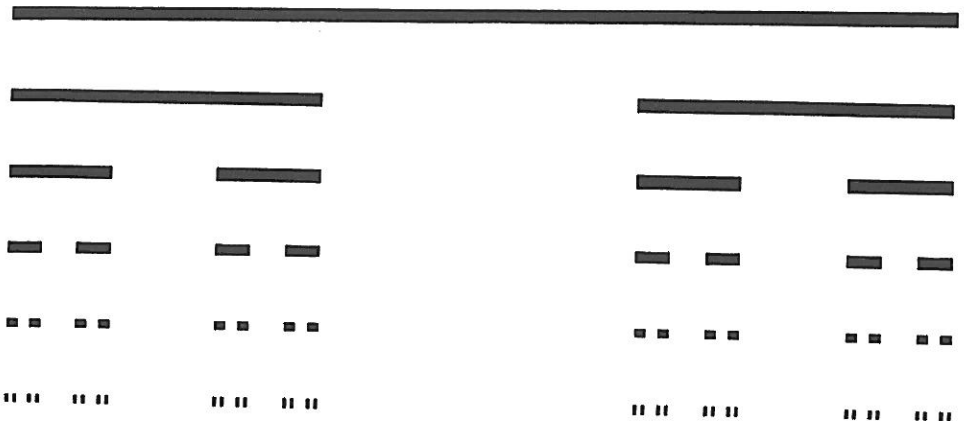

Figure 2.3. The triadic Cantor set shown in this figure is generated on the unit interval by replacing each of the intervals obtained at a given stage with two shorter ones.

The intervals or gaps between the points belonging to the fractal set correspond to the empty regions mentioned in Sec. 2.2. They are distributed according to a power law which is another typical property of fractals. In particular, for a Cantor set of dimension D the number of gaps longer than Δx_0 scales as $N(\Delta x > \Delta x_0) \sim \Delta x_0^{-D}$ (see rule g) in the previous section).

Example 2.2. One of the standard ways to construct a fractal surface is to replace the starting object with a single connected object of larger surface (made of reduced parts of the original one) and repeat this procedure using the reduced parts as originals. In two dimensions this method leads to a line (coastline) of infinite length with a fractal dimension larger than 1. Let us consider again the unit interval, and replace it with a curve consisting of 5 intervals of unit length as shown in Fig. 2.4. The fractal dimension is obtained from (2.10) and is equal to $D = \ln 5/\ln 3 \simeq 1.465$ which exactly coincides with D of the fractal shown in Fig. 2.1. and 2.2. In fact, the structure generated by this method is also analogous to that of Fig. 2.1.

Using a related procedure (Fig. 2.5) it is possible to define a single curve which can cover the unit square, i.e., it has a dimension equal to 2. For this so called Peano curve $D = \ln 9/\ln 3 = 2$, and in the limit of $k \to \infty$ it establishes a continuous correspondence between the straight line and the plane. The Peano curve is a very peculiar construction (it has

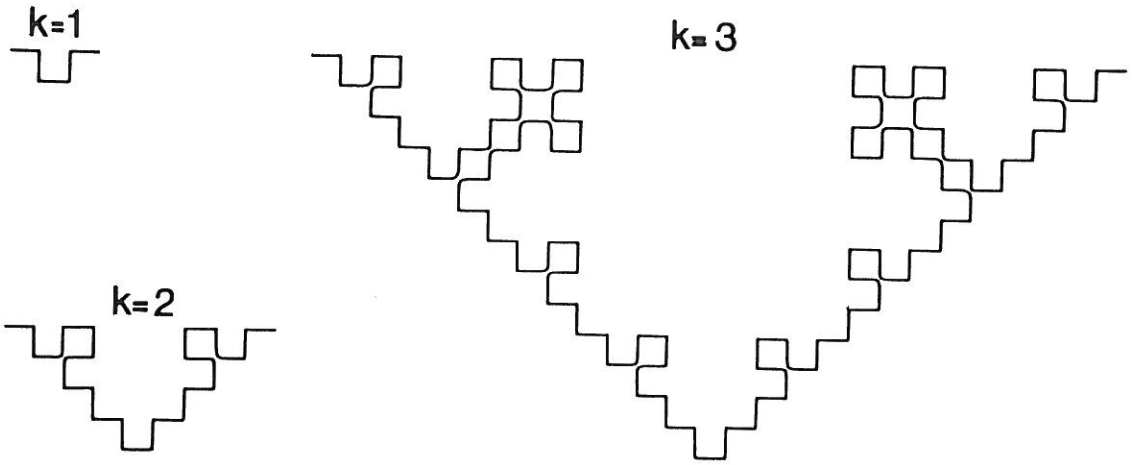

Figure 2.4. Construction of a growing fractal curve having the same fractal dimension as the objects shown in Figs. 2.1 and 2.2.

infinitely fine details being arbitrarily close to each other, but does not have any intersections), however, it is not a fractal according to the definition given in Sec. 2.2. This is indicated by the absence of empty regions.

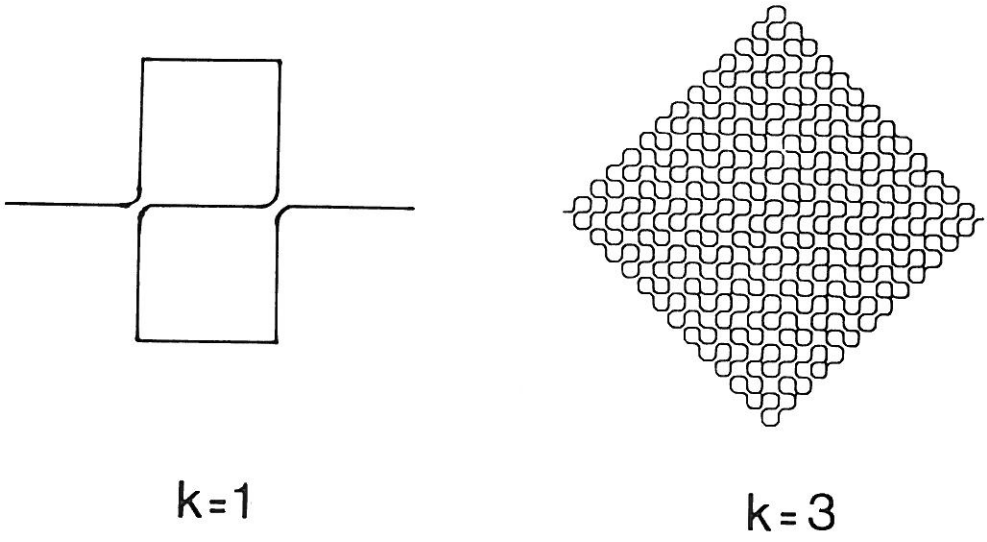

Figure 2.5. Application of Eq. (2.10) to the above displayed Peano curve gives $D = d = 2$ which means that this construction does not lead to a fractal according to the definition given in Section 2.2.

Example 2.3. The Sierpinski gasket shown in Fig. 2.6. is perhaps

the most studied two-dimensional fractal structure since it can be regarded as a prototype of fractal lattices with an infinite hierarchy of loops. When constructing this fractal, three of the four triangles generated within the triangles obtained in the previous step are kept. Since the linear size of the triangles is halved in every iteration, the fractal dimension of the resulting object is $D = \ln 3/\ln 2 \simeq 1.585$.

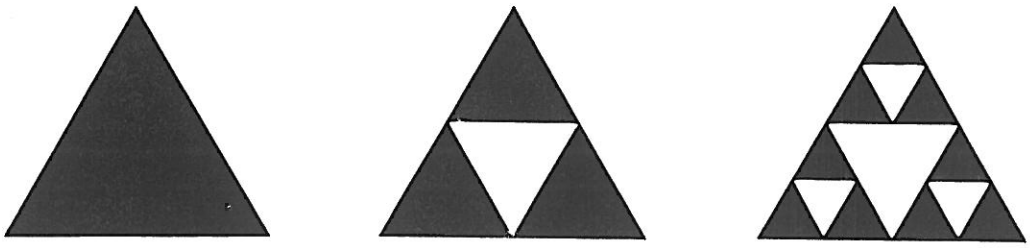

Figure 2.6. The Sierpinski gasket shown in this figure has loops on all length scales.

Example 2.4. The iteration procedure described at the beginning of this section is not the only possibility to construct mathematical fractals. For example, the Julia sets are derived from the transformation

$$z' = f(z) = z^2 - \mu, \tag{2.19}$$

where z and μ are complex numbers. The set of z values (points in the plane) which is invariant under the transformation (2.19) can be called self-squared, and for a fixed value of μ this set is in most of the cases a fractal, sometimes with a very attractive appearance (Peitgen and Richter 1986). (More precisely, Julia sets do not contain the stable fixed points of (2.19), i.e, they represent those points which can be obtained by backward iteration of (2.19)). 2.7 shows a few typical Julia sets.

Mandelbrot studied the convergence properties of the recursion

$$z_{k+1} = z_k^2 - \mu \tag{2.20}$$

corresponding to (2.19), as a function of μ. He found that the region of μ

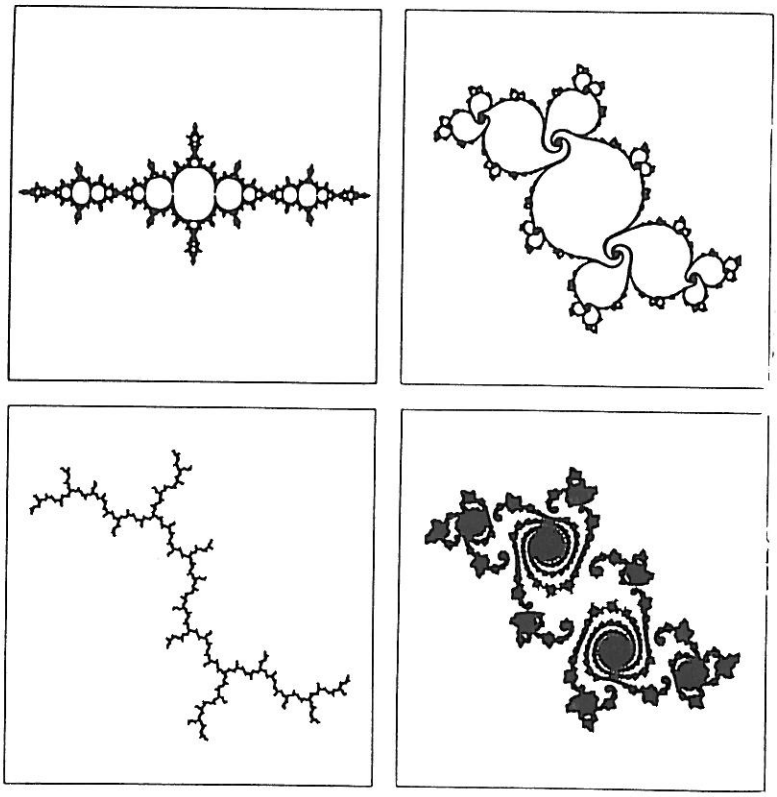

Figure 2.7. The rich variety of apparently self-similar Julia sets is well demonstrated by the above selected examples reproduced from Peitgen and Richter (1986).

values for which the iterates of $z_0 = 0$ under (2.20) fail to converge to ∞ (the Mandelbrot set) is bounded by a fractal curve (Fig. 2.9). Moreover, marking the points in the μ plane with colours depending on the number of iterations k needed for $z_k > 2$ one obtains an extremely complex, beautiful picture with many self-similar structures in it (Peitgen and Richter 1986).

Recursion relations are also used to construct fractal attractors characteristic of chaotic motion. As a simple example we briefly mention dynamical systems that period double on their way to chaos. At values $\lambda = \lambda_k$ the system gains a stable 2^k orbit. This series of period doublings accumulates at λ_∞, where the system follows a 2^∞ orbit. Such behaviour can be well represented by the following one-dimensional map

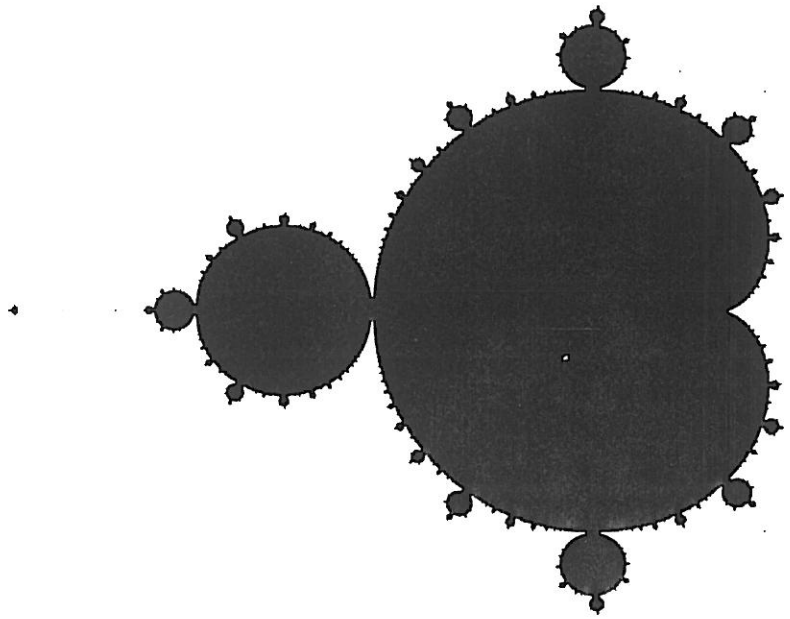

Figure 2.8. The region of μ values (Mandelbrot set) for which the iterates given by (2.20) remain finite for arbitrary k (Mandelbrot 1982).

$$x' = \lambda x(1 - x), \tag{2.21}$$

with $\lambda_\infty \simeq 0.837005134$. Here x is real and (2.21) is a one-dimensional counterpart of (2.19) in the sense that starting with some initial x_0 the calculated x' values quickly converge to a fractal subset of the $[0, 1]$ interval, i.e., this attractor is an invariant set corresponding to (2.21). However, the set invariant with regard to (2.19) is a repellor (not an attractor). It can be shown that the attractor forms approximately a non-uniform Cantor set (with $n = 2$ and $r_1 \neq r_2$). The fractal dimension of this set is $D \simeq 0.537$ (Hentschel and Procaccia 1983).

Example 2.5. The construction presented in Fig. 2.9 leads to a fractal which is both growing and non-uniform. To grow this fractal one adds to the four main tips of the already existing configuration a part of it in the following manner. The part to be added is the configuration itself minus one of the the main branches growing out from the centre vertically. Moreover, this part has to be rotated and reduced in an appropriate way

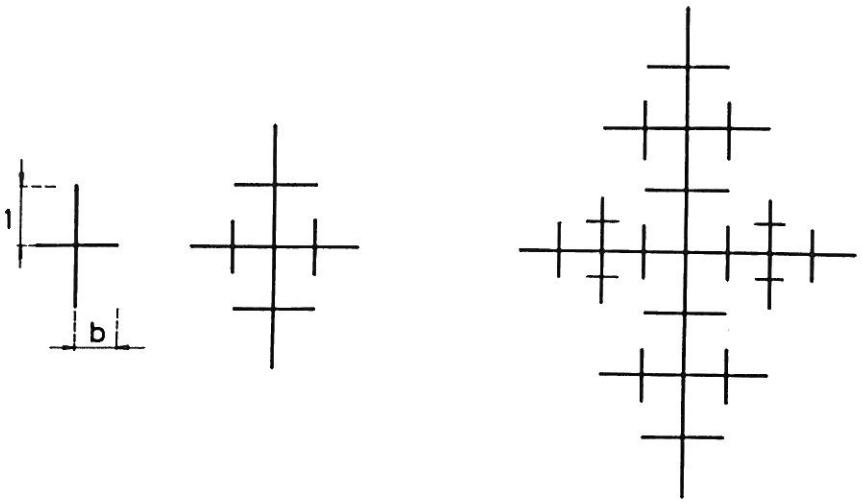

Figure 2.9. This non-uniform fractal grows by adding to the four principal tips of the $(n-1)$th configuration the structure itself without the lower main stem. This addition has to be done by applying appropriate rotation and shrinking to keep the ratio of the corresponding branches equal to $b < 1$.

(see Fig. 2.9) before attachment (reduction by a factor b is needed when the horizontal branches are updated).

To obtain the fractal dimension of this tree-like object we first note that reducing the configuration generated in the kth step by a factor 2^k one obtains a structure that would have been generated by the division technique with $1/r_1 = 1/r_2 = 1/2$ and $1/r_3 = 1/r_4 = b/2$ (replacing the intervals in each step with four new ones, two of which are half as long, and two with size shrunk by a factor $b/2$. Now we use (2.13) and calculate D from the equation

$$2\left(\frac{1}{2}\right)^D + 2\left(\frac{b}{2}\right)^D = 1 \tag{2.22}$$

which can be solved numerically for any given b. For some of the b values the implicit equation (2.22) can be inverted, e.g., if $b = 1/2$, $D = 1 - \ln(\sqrt{3} - 1)/\ln 2 \simeq 1.45$.

Example 2.6. The random motion of a particle represents a particularly simple example of stochastic processes leading to growing fractal

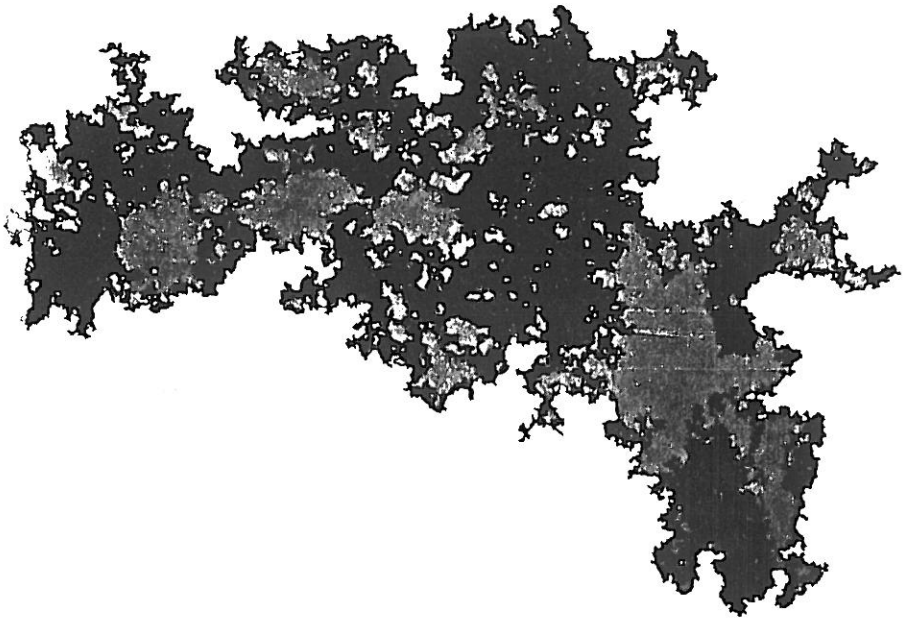

Figure 2.10. Example for a random coastline. This Brown hull represents the external perimeter of the trajectory of a looping random walk on the plane which is indicated by a darker line (Mandelbrot 1982).

structures. A widely studied case is when the particle undergoes a random walk (Brownian or diffusional motion) making steps of length distributed according to a Gaussian in randomly selected directions. Such processes can be described in terms of the mean squared distance $R^2 = \langle R^2(t) \rangle$ made by the particles during a given time interval t. For random walks $R^2 \sim t$ independently of d (see Chapter 5.) which means that the Brownian trajectory is a random fractal in spaces with $d > 2$. Indeed, measuring the volume of the trajectory by the total number of places visited by the particle making t steps, $(N(R) \sim t)$, the above expression is equivalent to

$$N(R) \sim R^2 \tag{2.23}$$

and comparing (2.23) with (2.2) we conclude that for random walks $D = 2 < d$ if $d > 2$. In this case, rather unusually, the fractal dimension is an integer number. However, the fact that it is definitely smaller than the embedding dimension indicates that the object must be non-trivially scale invariant.

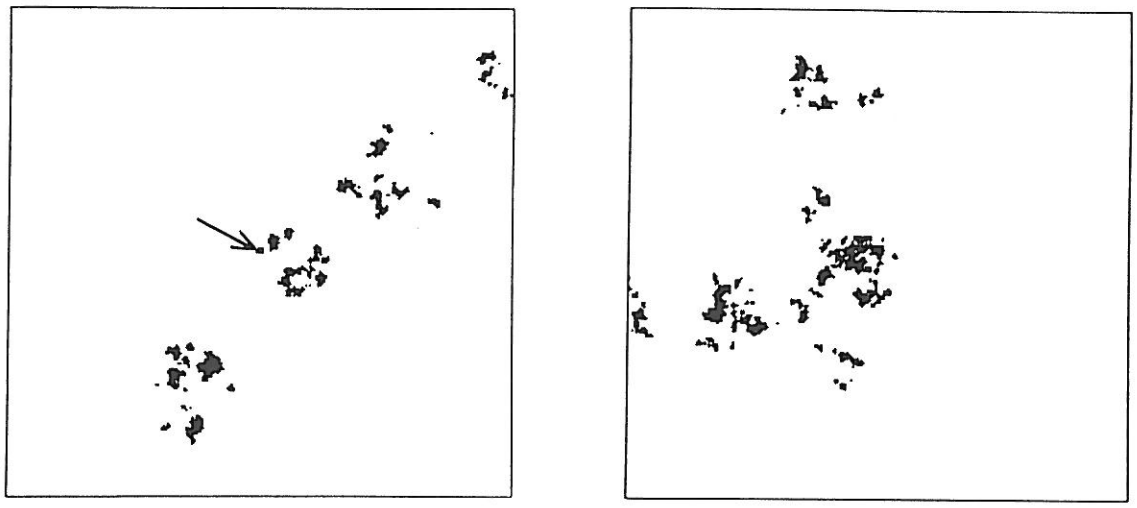

Figure 2.11. The shapes of disconnected clusters corresponding to the stopovers of a long Levy flight on the plane. The stochastic self-similarity of the clusters is demonstrated by blowing up small parts of the configurations. The picture on the right side is an approximately 100 times enlarged image of a tiny region in the left configuration indicated by the arrow (Mandelbrot 1982).

Brownian motion can be used to demonstrate random fractal curves in two dimensions as well. Consider the trajectory of a randomly walking particle on the plane. It separates the plane into two parts: an exterior which can be reached from a distant point without intersecting the trajectory and an interior (Fig. 2.10). The boundary of the interior part (the Brown hull) is a very complex curve resembling the coastlines mentioned earlier. According to the numerical results (Mandelbrot 1982) it is self-similar and has a dimension $D \simeq 4/3$ which is the same as that of self-avoiding random walks (see Section 5.4.2).

Example 2.7. A straightforward generalization of the Brownian motion is called Levy flight which is another example of growing random fractals. As before, it is a sequence of jumps in random directions, but with a hyperbolic distribution of the jump distances. More precisely, all directions are chosen with the same probability, and the probability of making a jump longer than Δx_0 is $Pr(\Delta x > \Delta x_0) = \Delta x_0^{-D_L}$, except that $Pr(\Delta x > \Delta x_0) = 1$ when $\Delta x_0 < 1$. All jumps are independent, and the resulting trajectory has a fractal dimension $D = D_L$.

Fig. 2.11 shows the positions of stopovers of a long Levy flight taking place on a plane. Most of the individual sites can not be seen for the given resolution. The displayed pattern is made of disconnected, but clustered positions, and was generated using $D_L = 1.26$ in the expression for the distribution of jump distances. The stochastic self-similarity of the configuration is manifested by the fact that enlarging a small part of the structure by about 100 times, the resulting configuration has the same general appearance as the original one.

2.3.2. Self-affine fractals

Self-similarity of an object is equivalent to the invariance of its geometrical properties under isotropic rescaling of lengths. In many physically relevant cases the structure of the objects is such that it is invariant under dilation transformation only if the lengths are rescaled by direction dependent factors. These anisotropic fractals are called self-affine (Mandelbrot 1982, 1985 and 1986).

Single-valued, nowhere-differentiable functions represent a simple and typical form in which self-affine fractals appear. If such a function $F(x)$ has the property

$$F(x) \simeq b^{-H} F(bx) \tag{2.24}$$

it is self-affine, where $H > 0$ is some exponent. (2.24) expresses the fact that the function is invariant under the following rescaling: shrinking along the x axis by a factor $1/b$, followed by rescaling of values of the function (measured in a direction perpendicular to the direction in which the argumentum is changed) by a different factor equal to b^{-H}. In other words, by shrinking the function using the appropriate direction-dependent factors, it is rescaled onto itself. For some deterministic self-affine functions this can be done exactly, while for random functions the above considerations are valid in a stochastic sense (expressed by using the sign $\simeq$).

Of course, there are self-affine fractals different from single-valued

functions and at the end of this section, among others, a couple of examples will be given for such structures as well. However, the most typical physical process producing self-affine structures is the marginally stable growth of interfaces (see Chapter 7.) leading to surfaces which can be well approximated by single-valued functions.

As we shall see self-affine fractals do not have a unique fractal dimension of the kind defined in Sec. 2.2. Instead, their global behaviour is characterized by an integer dimension smaller than the embedding dimension, while the local properties can be described using a local fractal dimension. To show this we shall concentrate on functions of a single scalar variable. Such a function is, for example, the plot of the distances measured from the origin, $X(t)$, of a Brownian particle diffusing in one dimension as a function of time t. It is obvious that a fractional Brown plot with $\langle X_H^2(t)\rangle \sim t^{2H}$ stochastically satisfies (2.24) by $F(t) = X(t)$.

Let us first construct a deterministic self-affine model, in order to have an object we can treat exactly (Mandelbrot 1985). The plot corresponding to this model, $M_H(t)$, is defined as a regular version of the above mentioned Brown plot. We assume that H is of the form

$$H = \ln b_2 / \ln b_1, \tag{2.25}$$

where b_1 and b_2 are integers and $b_1 - b_2 > 0$. The idea is that the function $X_H(t)$, whose increments are Gaussian over all δt with a standard deviation $(\delta t)^H$, is replaced by a function $M_H(t)$ whose increments over suitable δt-s are binomial with the same mean equal to 0 and the same standard deviation. This means that we require

$$M_H(pb_1^{-k}) - M_H[(p+1)b_1^{-k}] = \pm(b_2)^{-k} = \pm(\delta t)^H \tag{2.26}$$

for all k and p, where (2.25) was used to get the last equality for $\delta t = b_1^{-k}$.

An actual construction of such a bounded self-affine function on the unit interval is demonstrated in Fig. 2.12. In this example $b_1 = 4$ and

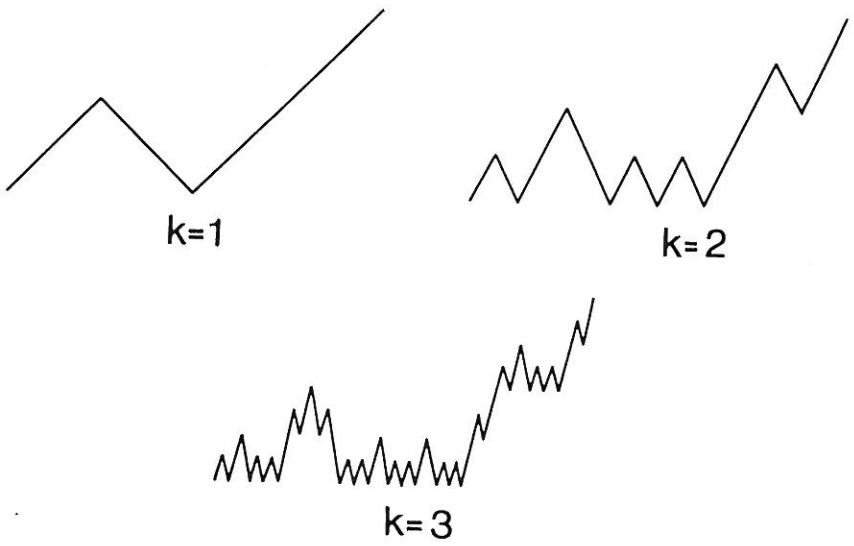

Figure 2.12. Deterministic model for a self-affine function defined on the unit interval. The single-valued character of the function is preserved by an appropriate distortion of the z-shaped generator ($k = 1$) of the structure.

$b_2 = 2$. The object is generated by a recursive procedure by replacing the intervals of the previous configuration with the generator having the form of an asymmetric letter z made of four intervals. However, the replacement this time should be done in a manner different from the earlier practice. Here every interval is regarded as a diagonal of a rectangle becoming increasingly elongated during the iteration. The basis of the rectangle is divided into four equal parts and the z-shaped generator replaces the diagonal in such a way that its turnovers are always at analogous positions (at the first quarter and the middle of the basis). In the kth stage we obtain $M_H^{(k)}(t)$, and the function becomes self-affine in the $k \to \infty$ limit.

Now we can apply an exact argument to determine the structure's local dimension using definition (2.5) which with $l = 1/b$ reads as $D = \lim_{b\to\infty} \ln N(b)/\ln b$ where $N(b)$ is the number of discs or boxes of linear size $1/b$ needed to cover the object. Let us cover $M_H(t)$ from $t = 0$ to $t = 1$ with boxes of size $1/b = b_1^{-k}$. For this purpose one needs $b_1^k = b$ bins or columns of boxes. The height of these columns (the amount by which $M_H(t)$ changes in an interval of length b_1^{-k} is approximately b_2^{-k}, because of (2.26).

Consequently, to cover $M_H(t)$ in a bin one needs (b_2^{-k}/b_1^{-k}) boxes. The number of boxes needed along the whole unit interval is

$$N(b) \sim b_1^k \left(\frac{b_2^{-k}}{b_1^{-k}} \right) = (b_1^2 b_2^{-1})^k. \tag{2.27}$$

From (2.25) we have $b_2 = b_1^H$, hence $N(b) \sim b^{2-H}$ which according to (2.5) leads to

$$D_B = 2 - H, \tag{2.28}$$

where D_B denotes the *local or box dimension* of the plot of $M_H(t)$.

To show the validity of the statement that the global dimension of an unbounded self-affine function is equal to 1 we slightly modify the construction of the previously introduced deterministic example. This new version has to be defined for $t \gg 1$, but have the same scaling properties on the unit interval as $M_H(t)$. We construct the kth stage of the new function $\tilde{M}_H^{(k)}(t)$ from $M_H^{(k)}(t)$ by expanding it along the t axis and multiplying its values by an appropriate factor

$$\tilde{M}_H^{(k)}(t) \sim \left(\frac{b_1}{b_2} \right)^{kH} M_H^{(k)} \left[\left(\frac{b_1}{b_2} \right)^{-k} t \right].$$

On the unit interval $\tilde{M}_H(t)$ behaves as $M_H(t)$ because of the self-affine property (2.24), therefore, it has the same local fractal dimension $2-H$ (2.28). The values of this new function are now defined up to $t \to \infty$ as $k \to \infty$, moreover, its largest value in this limit diverges as t^H with $H < 1$ (slower than t). This leads to the conclusion that the *global dimension*, D_G, determined for the structure in the limit of large t using boxes of size $1/b \gg 1$ is equal to 1. In this case "observing the function from a large distance" (measuring with large boxes) it looks like a ragged line nearly merged into the abscissa.

We have seen that by rescaling a bounded self-affine function, or in other words, changing the units in which the distances are measured, an extra

dimension, called global dimension could be found. This raises the question of choosing the appropriate units to measure F and t. To see both the local and global behaviours one should make a choice for the unit of both F and t. Then a quantity t_c can be defined through

$$|F(t+t_c) - F(t)| \sim |t_c|. \tag{2.29}$$

This t_c can be called the *crossover scale* for the given process. The most essential fact about t_c is that it depends on the units which happen to be selected for F and t, therefore, the position of the crossover is in general not intrinsic.

An *important consequence* of the above statement is that for self-affine structures with a lower or upper length scale, changing the units may lead to losing the possibility of detecting the local fractal or the global trivial scaling. Indeed, if the units we chose are such that t_c becomes the same order as the lower cutoff length, a local fractal dimension can not be observed. This is the case, e.g., for the record of a one-dimensional random walk on a lattice if the same unit is used for the increments of F and the time t, since then the lower cutoff and the crossover scale coincide. Similar arguments are valid for the detectability of a trivial global dimension.

Before the discussion of additional examples it should be noted that the most typical self-affine structures (and the ones we consider) are diagonally self-affine. This means that they are invariant under a transformation whose invariant sets include any collection of straight lines parallel to the coordinate axes. A diagonal affine transformation is specified by giving a fixed point of coordinates φ_m $(0 < m < d-1)$ and an array of reduction ratios r_m, and considering the map

$$x_m \rightarrow \varphi_m + r_m(x_m - \varphi_m). \tag{2.30}$$

The ratios r_m must not be equal, because then the transformation would be isotropic. The most general kind of self-affinity would imply invariance with regard to a transformation whose matrix has off diagonal elements as well.

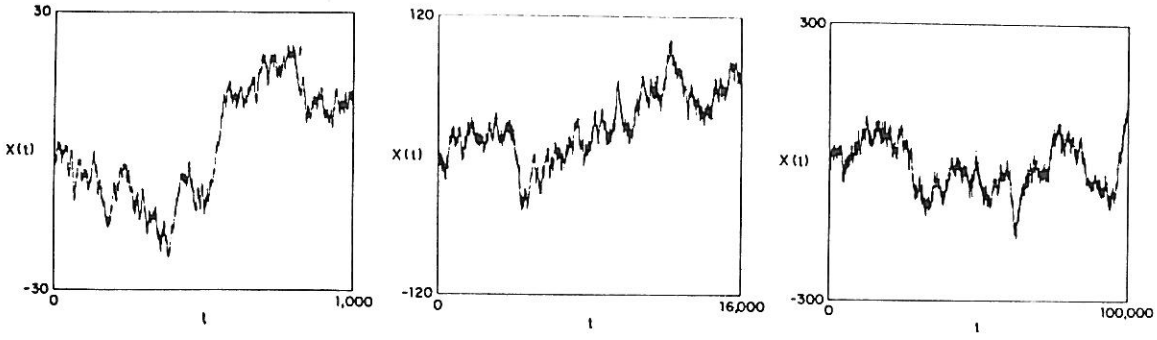

Figure 2.13. These plots of $X_{1/2}(t)$ were obtained by rescaling of Brownian plots of various lengths. For each of the three plots the vertical scale is proportional to the square root of the horizontal scale (Meakin 1986).

EXAMPLES

Example 2.8. It is possible to treat the random function $X_H(t)$ in a manner analogous to the approach which was used for the description of the deterministic function $M_H(t)$, however, the arguments in this case involve heuristic approximations. We recall that $X_H(t)$ denotes the distance of a particle from the origin, randomly walking on a straight line, as a function of the time t. The distances are measured from the starting point, the direction of the jumps is chosen randomly (but not necessarily independently), and it is assumed that the mean squared distance scales with time according to

$$\langle X_H^2(t)\rangle \sim t^{2H}. \tag{2.31}$$

A random walk of this kind with $0 < H \neq 1/2 < 1$ is called fractional Brownian motion in one dimension. It is well known that for the ordinary Brownian motion, when the jumps are independent and their distances have a Gaussian distribution, $H = 1/2$ (i.e., $D_B = 2 - H = 1.5$) and $X_{1/2}(t)$ satisfies (2.24) stochastically. Similarly, $X_H(t)$ and $b^{-H}X_H(bt)$ can be shown to be identical in distribution.

Fig. 2.13 visualizes the statistical self-affinity of the Brown plot with

$H = 1/2$. Parts of originally different horizontal extension are scaled onto the same interval with a simultaneous rescaling of the heights by a factor which is equal to the square root of the factor used to shrink the horizontal size. The plots obtained are very similar as far as their appearance is concerned.

Since $0 < H < 1$, it follows from (2.31) that the global dimension corresponding to the behaviour for $t_c \gg 1$ is 1, because $X_H(t)/t \to 0$ as $t \to 0$. The local dimension can be obtained from considerations similar to those used for the deterministic case. During a time interval δt, $|max\ [X_H(t)] - min\ [X_H(t)]|$ is of the order of $(\delta t)^H$. Covering the part of $X_H(t)$ on the interval δt by squares of side δt requires on the order of $(\delta t)^H/\delta t = \delta t^{H-1}$ squares. Therefore, covering $X_H(t)$ on the interval $[0,1]$ requires

$$N(\delta t) \sim \frac{\delta t^{H-1}}{\delta t} = \delta t^{-(2-H)} \tag{2.32}$$

which according to the definition (2.5) leads to $D_B = 2 - H$ just as for the deterministic construction (see Eq. 2.28).

The points at which $X_H(t) = 0$ form the zero set of the fractional Brownian motion. It is a random Cantor set of fractal dimension $D = 1 - H$ (Mandelbrot 1982). A fractional Brownian motion with $0 < H < 1/2$ is antipersistent which means that the walker tends to turn back to the point it came from. Alternatively, in the case $H > 1/2$ the increments have positive correlation with the direction of the previous jump. To see this we set $X_H(0) = 0$ and define the past increment as $-X_H(-t)$ and the future increment as $X_H(t)$. Then

$$\begin{aligned} \langle -X_H(-t)X_H(t)\rangle &= 2^{-1}\{\langle [X_H(t) - X_H(-t)]^2\rangle - 2\langle [X_H(t)]^2\rangle\} = \\ &= 2^{-1}(2t)^{2H} - t^{2H}. \end{aligned} \tag{2.33}$$

Dividing by $\langle X_H^2(t)\rangle = t^{2H}$, one obtains the correlation of increments which is independent of t; it is equal to $2^{2H-1} - 1$ vanishing, as expected, for $H = 1/2$. Calculating the Fourier spectrum of a fractional Brown function one finds that the coefficients of the series, $A(f)$, are independent Gaussian random variables and their absolute value scales with the frequency f according to a

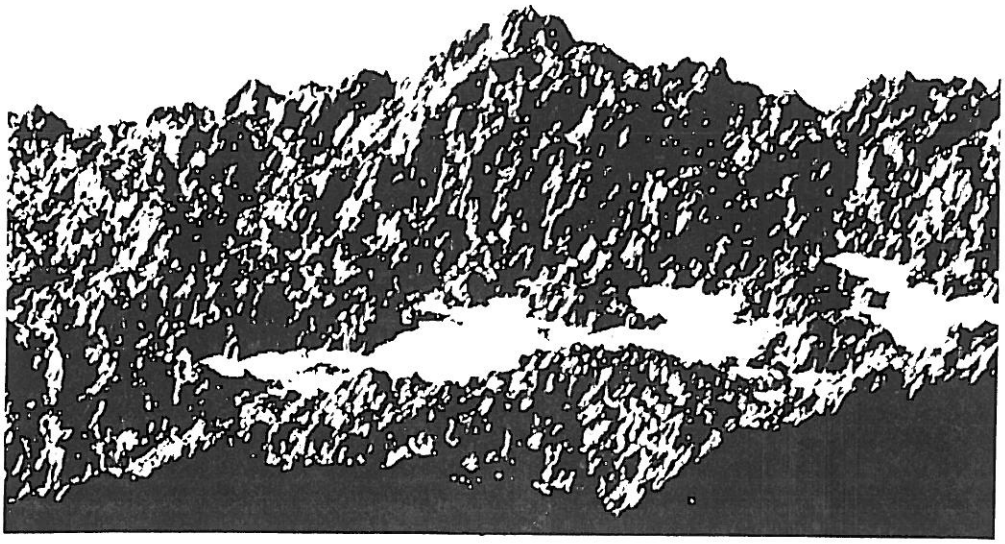

Figure 2.14. A Brownian surface having a local fractal dimension close to 2.4 (Mandelbrot 1982).

power law

$$|A(f)| \sim f^{-H-\frac{1}{2}}. \tag{2.34}$$

Finally, as an example for random self-affine functions defined in higher dimensional spaces we mention the Brownian relief or Brown plane-to-line function shown in Fig. 2.14. Its vertical cross sections represent plots of one dimensional random walks $(X_H(t))$. It is not a trivial task to define and construct a fractional Brownian surface with a given H. There is, however, a relatively simple procedure generating a surface in $d = 3$ with $H = 1/2$. A horizontal plateau is broken along a straight line chosen at random and one of them shifted verically. The difference between the levels of the two sides of the resulting precipice is also chosen randomly from a set of lengths distributed according to a Gaussian. Then we repeat the same and follow the kth stage by dividing all heights by $\sqrt{k}$. Generating surfaces with an arbritrary H requires other methods, e.g. involving the construction of a set of random Fourier coefficients with a distribution $f^{-H-3/2}$ and reconstructing the surface from its components or random addition algorithms (Voss 1985).

Example 2.9 In 1872 Weierstrass constructed a function which is continuous everywhere, but differentiable nowhere. Mandelbrot proposed a simple extension of this function which turned out to have no characteristic length scale. Let us consider the Fourier series

$$C(t) = \sum_{n=-\infty}^{\infty} \frac{1 - \cos(b^n t)}{b^{(2-D)n}}, \tag{2.35}$$

which is the real part of the more general Weierstrass-Mandelbrot function (Mandelbrot 1982). In the range of parameter values

$$1 < D < 2, \qquad b > 1 \tag{2.36}$$

$C(t)$ is continuous but the series defining $dC(t)/dt$ diverges everywhere. The frequencies b^n form a "Weierstrass spectrum", spanning the range from zero to infinity in a geometrical progression; this is the sense in which $C(t)$ possesses no scale. The self-affinity of $C(t)$ for $b > 0$ can be easily shown by a formal replacement of n by $n + 1$ in (2.35) leading to the scaling relation $C(t) = b^{-(2-D)} C(bt)$ which is equivalent to the definition (2.24) of self-affine functions. This means that the graph of $C(t)$ on the interval $t_0 \leq t \leq bt_0$ can be obtained by magnifying the graph in the range $t_0/b \leq t \leq t_0$ with factors b and b^{2-D} in horizontal and vertical directions, respectively.

It can be argued and supported by numerical investigations that the local fractal dimension of $C(t)$ is equal to the parameter D. Consequently, for $D = 1.5$ it may also be regarded as a deterministic model for Brownian motion.

Example 2.10 So far we have discussed single-valued self-affine functions, because they seem to be more relevant from the point of view of applications than other possible self-affine structures. The two examples given below represent other types of self-affine objects, constructed in a spirit related to that used to generate some of the self-similar fractals.

Fig. 2.15 shows a growing structure which is a generalization of the fractal displayed in Fig. 2.1a. The rules of construction are analogous, but

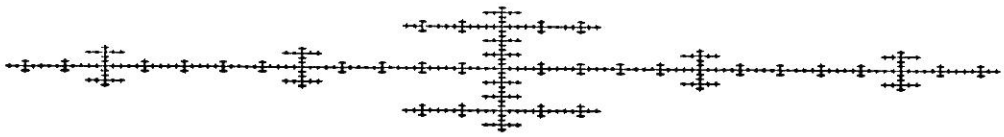

Figure 2.15. This growing self-affine fractal is generated by a procedure analogous to that used for constructing Fig. 2.1a, except that in the present case the seed configuration is not isotropic (Jullien and Botet 1987).

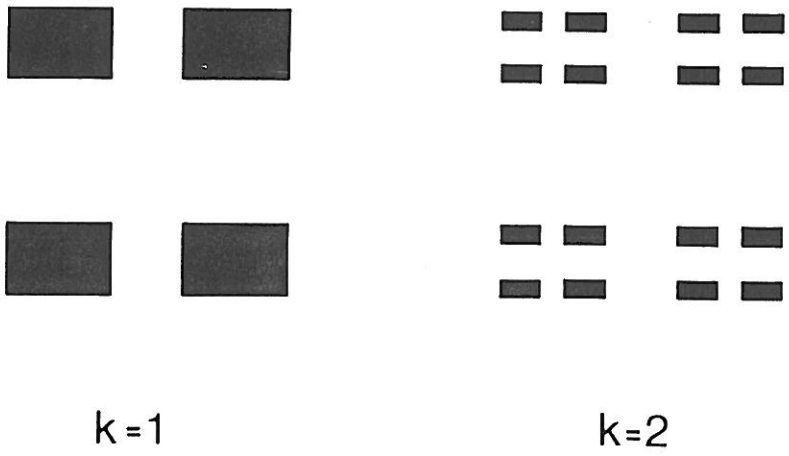

Figure 2.16. Generating a disconnected self-affine fractal embedded into two dimensions using elongated rectangles instead of squares during its construction.

in the present case the seed configuration is anisotropic (Jullien and Botet 1987). As before, the self-affine structure is produced in the $k \to \infty$ limit, and the kth configuration is obtained by replacing the 7 subunits of the $k-1$th configuration with the whole structure generated in the $k-1$th step. Obviously, the global dimension of the resulting object will be equal to 1, since the width of the structure grows with k as 3^k, while its length as k^5. This self-affine fractal has a lower cutoff length which is the size of the particles it is made of, therefore, *it has no local fractal dimension.*

The last example of this section is constructed by dividing the unit square into anisotropic subunits which serve as seeds for further divisions.

Fig. 2.16 demonstrates the actual procedure analogous to that used for generating the fractal shown in Fig. 2.1b. For this example the scales are chosen in such a way that the crossover scale is the same as the side of the unit square, and because of this the trivial global scaling is not manifested (although it could be seen by applying the constructon "backward", i.e., growing the square). On the other hand, the structure has a local fractal dimension which can be calculated, for example, by covering the structure with squares of size corresponding to the shorter side of the elongated rectangles generated at each step of the construction. One can also use rule d) of Section 2.2. Let us assume that in the kth step the sides of the rectangles are $l_1^{(k)} = l_1^k$ and $l_2^{(k)} = l_2^k$, where $l_1 < l_2$. Since the fractal shown in Fig. 2.16 can be generated by multiplying two Cantor sets of dimensions $D_1 = \ln 2/\ln(1/l_1)$ and $D_2 = \ln 2/\ln(1/l_2)$, respectively, we obtain for the local fractal dimension of the resulting structure $D_L = \ln 2/\ln(1/l_1) + \ln 2/\ln(1/l_2)$.

2.3.3. Fat fractals

The most important feature of structures discussed in the previous sections was that they had a fractal dimension strictly smaller than the embedding dimension d. There are, however, structures for which $D = d$, but still exhibit a fractal behaviour (Mandelbrot 1982) in the following sense. When one calculates the volume $V(l)$ of such fat fractals using balls of decreasing size l, it *converges to a finite value algebraically* with a noninteger exponent. This is in contrast to ordinary or thin fractals, where $V(l) \to 0$ if $l \to 0$.

In general, the resolution dependent volume of an object can be written in the form

$$V(l) = V(0) + f(l), \tag{2.37}$$

where $V(0) = V_0$ is the volume in the limit $l \to 0$. For thin (ordinary) fractals $V(0)$=0, and $f(l) \sim l^{d-D}$ with $D < d$. For fat fractals $V(0) > 0$, but $f(l)$ - as in the case of the thin ones - follows a power law with an exponent which can be regarded as a quantity characterizing the scaling properties of the structure. This fact can be expressed in the form (Farmer 1986)

$$V(l) \simeq V(0) + Al^{\beta} \tag{2.38}$$

where A is a constant and β is an exponent quantifying fractal properties. β can be calculated from

$$\beta = \lim_{l \to 0} \frac{\ln[N(l)l^d] - V(0)}{\ln l}, \tag{2.39}$$

where $N(l)$ is the number of d-dimensional balls needed to cover the structure. By definition $\beta > 0$, and it is equal to ∞ for non-fractal sets.

It is important to note that fat fractals are in general not self-similar objects. They have more in common with the Peano curve, since these structures are typically made of parts with dimension smaller than the embedding dimension d, while the whole object has a finite measure in d (lines with positive area, surfaces with positive volume, etc.). However, fat fractals are more inhomogeneous than the Peano-type objects, since for the latter $V(l)$ converges exponentially to its limiting value.

The example to be discussed below is constructed by generalizing the procedure leading to Cantor sets. However, there are many physical systems in which fat fractals are expected to occur. It has been shown that fat fractals can be associated with chaotic parameter values beyond the period-doubling transition to chaos, chaotic orbits of Hamiltonian systems or ballistic aggregation clusters. In addition, such biological objects as bronchia in the lung or coral-colonies are most likely to have the structure of fat fractals.

EXAMPLES

Example 2.11 As an illustration of fat fractals, consider the following modified Cantor set. In the original version (Example 2.1) first the central third of an interval is deleted, then the central third of the remaining intervals and so on *ad infinitum*. To "fatten" this thin fractal delete instead the central $\frac{1}{3}$, then $\frac{1}{9}$, then $\frac{1}{27}$, etc., of each remaining interval. The resulting set is

topologically equivalent to the classical Cantor set, but the holes decrease in size sufficiently fast so that the limiting set has nonzero Lebesque measure and a dimension equal to 1.

The exponent β can be easily computed for the more general case of cutting out intervals of length $h_k(c) = c^k$ at stage k, where $0 < c < 1$ is a parameter (Umberger *et al* 1986). For a given c the total length (Lebesque measure) of the remaining set is larger than zero and is given by $0 < L_\infty = lim_{n\to\infty} L_n < 1$, where

$$L_n = N_n \epsilon_n = 2^n \epsilon_n. \tag{2.40}$$

In the above expression the length of the covering intervals is chosen to be equal to the length of a single segment after the nth iteration is completed

$$\epsilon_n = \frac{1}{2^n} \prod_{k=1}^{n} (1 - c^k). \tag{2.41}$$

To calculate β for this set we use (2.39)

$$\begin{aligned} \beta &= \lim_{n\to\infty} \frac{\ln(L_n - L_\infty)}{\ln \epsilon_n} \\ &= \lim_{n\to\infty} \frac{\ln[1 - \prod_{k=n+1}^{\infty} (1 - c^k)]}{n \ln(1/2)} \end{aligned} \tag{2.42}$$

where the terms $\prod_k^n (1 - c^k) = o(n)$ are not written out. The above limit can be evaluated by using the identity $\ln\left[\prod(1 - c^k)\right] = \sum \ln(1 - c^k)$ to give

$$\beta = \frac{\ln(1/c)}{\ln 2}. \tag{2.43}$$

This example can be extended to arbitrary embedding dimension (Mandelbrot 1982). Suppose that we cut out a piece of volume v_1 from the unit hypercube of dimension d in such a way that the resulting structure is made of the 2^d hypercubes remaining at the corners of the starting object.

Next, from each of these cubes a similar piece of relative volume v_2 is cut out, and this process is repeated infinitely many times. The total volume remaining after the kth iteration is

$$V_k = (1 - v_1)(1 - v_2)...(1 - v_k) = \prod_0^k (1 - v_k). \tag{2.44}$$

V_k decreases as $k \to \infty$ to a limiting value V. For v_k fixed one has $V = 0$, however, if $\sum_0^\infty v_k < \infty$, the limiting volume is positive, $\prod_0^\infty (1 - v_k) > 0$. Since these objects are inhomogeneous in a rather specific way, measuring their volume with balls of size l one finds that it converges to $V(0) = V$ according to (2.38).

Example 2.12 To construct a fat fractal having a structure more typical for growth phenomena than Cantor sets, one can modify the method discussed in Example 2.5. In its original form the tree-like object shown in Fig. 2.9 is a thin fractal with a fractal dimension depending on b, which is the length ratio of the first horizontal and vertical branches. It is obvious from the construction as well as from (2.22) that $b = 1$ results in a two-dimensional, "homogeneously fat" object for which $f(l)$ converges to zero exponentially fast. In order to generate an inhomogeneous fat fractal one should select a sequence of b_k values such that $\sum_0^\infty (1 - b_k) < \infty$.